AJNR

Three-dimensional time-of-flight MR angiography in the evaluation of intracranial aneurysms treated by endovascular balloon occlusion.

J S Tsuruda, R J Sevick and V V Halbach

AJNR Am J Neuroradiol 1992, 13 (4) 1129-1136
http://www.ajnr.org/content/13/4/1129

Three-Dimensional Time-of-Flight MR Angiography in the Evaluation of Intracranial Aneurysms Treated by Endovascular Balloon Occlusion

Jay S. Tsuruda, Robert J. Sevick,[1] and Van V. Halbach

Summary: The authors share their experience with MRA in the assessment of cerebral aneurysms. Despite its limitations—spatial resolution, insensitivity to slow flow states, subacute thrombus artifacts—they believe the technique shows potential.

Index terms: Arteries, cerebral; Veins, cerebral; Aneurysms, arteriovenous; Magnetic resonance angiography (MRA)

First described by Serbinenko in 1974 (1), endovascular balloon occlusion (EBO) has been used primarily in the treatment of intracranial aneurysms and arteriovenous malformations. Using detachable balloons for permanent proximal arterial occlusion, Fox et al reported complete aneurysm occlusion in 65 of 67 patients (2). Higashida et al report complete aneurysm occlusion in 65 of 84 patients using direct balloon placement within the aneurysm (3).

At our institution, follow-up of patients with intracranial aneurysms treated by EBO includes both serial clinical examinations as well as plain radiographs, x-ray angiography (XRA), computed tomography (CT), and spin-echo (SE) magnetic resonance (MR) imaging. The objectives of the imaging studies are: to determine whether residual flow is present either in the parent artery or aneurysm, to assess intraluminal thrombus, and to demonstrate the position of occluding balloons. While these objectives are met by XRA in most cases, a noninvasive alternative is desirable.

Preliminary studies indicate the potential utility of three-dimensional time-of-flight (3DTOF) magnetic resonance angiography (MRA) (4, 5) in the evaluation of untreated intracranial aneurysms (6–8). Our initial experience in five patients with treated aneurysms will be described.

Case Report

Patient 1

A 58-year-old woman presented with an 8-mm left supraclinoid internal carotid artery aneurysm 45 months ago. Surgical clipping was attempted but was unsuccessful. The patient subsequently underwent EBO using a single detachable balloon placed within the aneurysm lumen with preservation of the flow within the parent artery. The imaging findings are shown in Figure 1. A follow-up XRA (Fig. 1A) demonstrates residual aneurylumenal filling. The SE MR and MRA (Figs. 1B–1E) were obtained 17 months following the XRA. Because of the good correlation between the XRA and MRA in demonstrating no significant change in the lumen size and because the patient was currently asymptomatic, it was elected not to perform a follow-up XRA or further therapy at this time.

Patient 2

A 45-year-old woman presented with multiple 8- to 10-mm aneurysms involving the right cavernous and supraclinoid internal carotid artery. The patient was treated by EBO with placement of a single balloon within the supraclinoid aneurysm lumen and two balloons within the cavernous carotid artery. The immediate postoperative angiogram (data not shown) demonstrated complete occlusion of the parent artery and nonfilling of both aneurysms. Six months later, the follow-up CT (Fig. 2A) demonstrated questionable enhancement of a residual lumen. However, the SE MR and MRA (Figs. 2B and 2C) showed no definite evidence of abnormal flow. Therefore, a repeat XRA was not performed.

Patient 3

A 51-year-old woman underwent SE MR and MRA 40 months following parent artery EBO for a 5-mm right supraclinoid internal carotid artery aneurysm. At the time of right internal carotid artery occlusion, the patient was

Received June 17, 1991; accepted and revision requested September 8; revision received October 10. All authors: Department of Radiology, Diagnostic and Interventional Neuroradiology Section, Box 0628, University of California, San Francisco, CA 94143-0628. Address reprint requests to J. S. Tsuruda, MD: present address: Department of Radiology, SB-05, University of Washington, Seattle, WA 98195.

[1] Supported by a clinical fellowship from the Alberta Heritage Foundation for Medical Research.

AJNR 13:1129–1136, Jul/Aug 1992 0195-6108/92/1304-1129

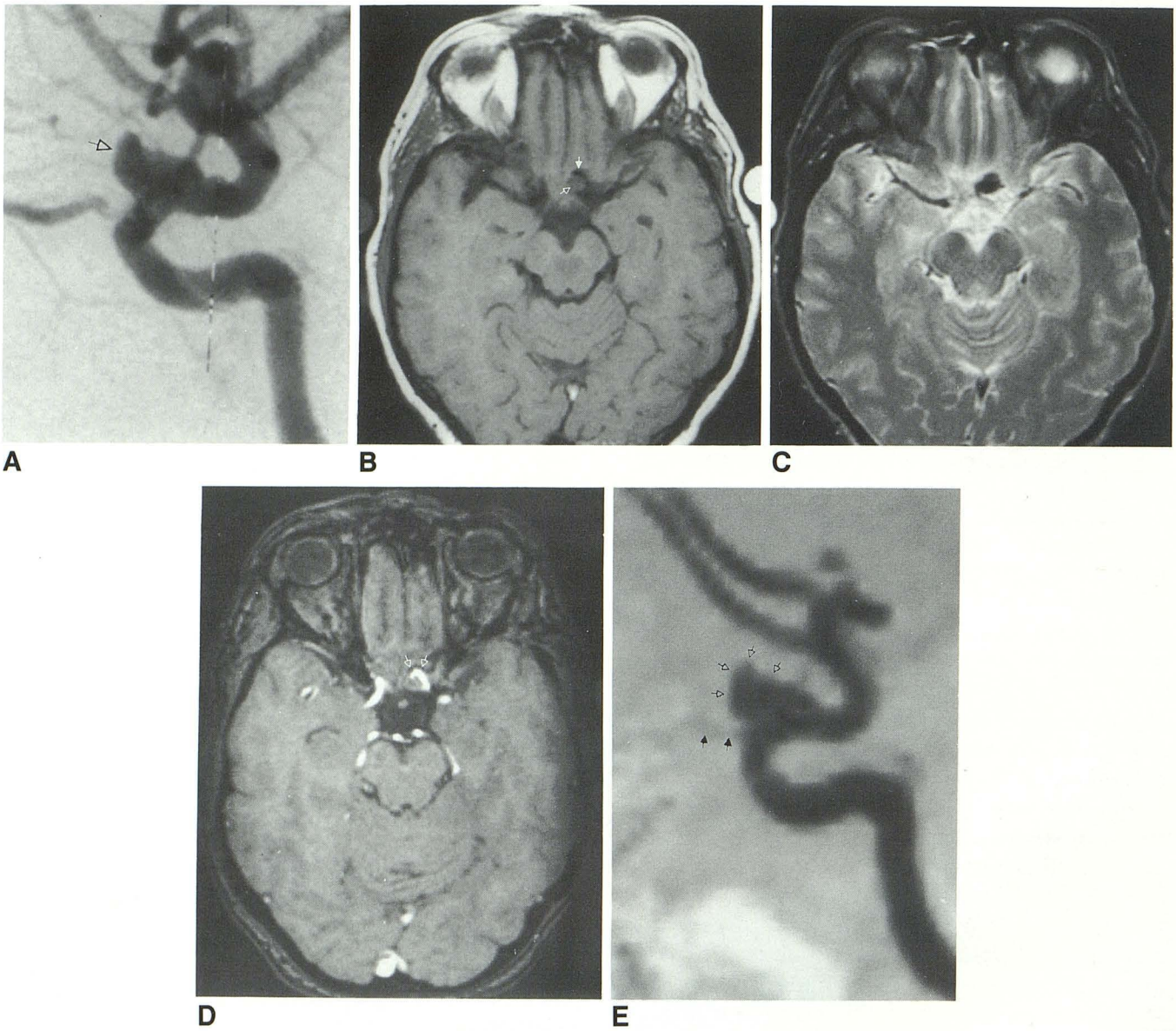

Fig. 1. A 58-year-old woman (patient 1) with a left supraclinoid internal carotid artery aneurysm. This example shows the potential of MRA in obtaining comparable results when compared to XRA in depicting residual aneurysm lumenal filling, as well as localization of the occlusion balloon.

A, Left lateral XRA of the internal carotid artery demonstrates residual filling of the aneurysm lumen (*arrow*).

B, Axial T1-weighted (600/20) spin-echo image shows intermediate signal intensity occluding balloon (*open arrow*). An area of signal void (*solid arrow*) is seen anterolaterally, which could represent flow, hemosiderin, or calcification.

C, Axial T2-weighted (2800/80) spin-echo image. Occluding balloon is now hypointense, simulating flow-related signal void.

D, Axial partition from MRA demonstrates intermediate signal intensity occluding balloon. A crescentic area of high signal flow-related enhancement (*open arrows*) is seen anterolaterally, representing residual blood flow within the aneurysm.

E, Lateral MRA reprojected view of the left internal carotid artery shows residual aneurysm lumen (*open arrows*) projecting anteriorly just distal to origin of a faintly visualized ophthalmic artery (*solid arrows*). The causes for poor visualization of the ophthalmic artery on MRA are noted in the discussion.

also noted to have a partially thrombosed left carotid-ophthalmic artery aneurysm that was not treated (Fig. 3A). The follow-up MRA confirmed occlusion of the right internal carotid artery and nonfilling of the right supraclinoid aneurysm (Fig. 3B), as well as the lack of interval change of the left internal carotid aneurysm (Fig. 3C). Because of the unchanging imaging findings, a repeat XRA was not performed.

Patient 4

A 60-year-old man was evaluated 31 months after intraaneurysmal balloon occlusion of a basilar tip aneurysm, using three balloons. The XRA immediately following EBO demonstrated a small aneurysmal remnant (Fig. 4A). The follow-up SE MR (Figs. 4B and 4C) demonstrated heterogeneity of signal intensity between the various bal-

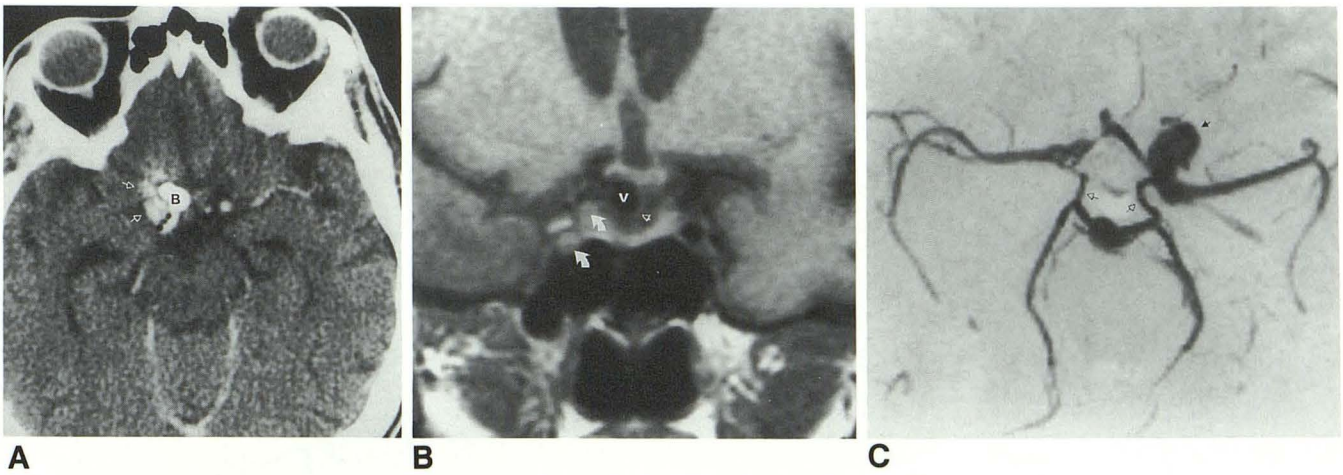

Fig. 2. A 45-year-old woman (patient 2) with both intraaneurysmal and parent artery balloon occlusion for multiple right internal carotid artery aneurysms 6 months before MRA. This example demonstrates the utility of MRA in confirming the occlusion of the parent right internal carotid artery and in the evaluation of the patency of the remaining circle of Willis.

A, Axial contrast-enhanced CT scan shows hyperdense occluding balloon (*B*) surrounded by a periphery of contrast enhancement (*open arrows*). This enhancement either represents contrast filling residual lumen or enhancing thrombus.

B, Coronal T1-weighted (600/20) spin-echo image shows an area of signal void (*v*) in the right suprasellar cistern with mass effect on the infundibulum (*open arrow*). This region of signal void was thought to represent either the intraaneurysmal occluding balloon or vascular flow void due to the presence of a patent residual aneurysm lumen. Note the lack of flow void in the occluded ipsilateral internal carotid artery (*curved arrows*).

C, Submental vertex MRA collapsed view demonstrates the lack of flow-related enhancement in the suprasellar cistern. There is visualization of the distal supraclinoid segment of the right internal carotid artery, as well as the proximal segments of the anterior and middle cerebral arteries. Note the patent left internal carotid artery (*solid arrow*) that was noted to be normal on additional projections (data not shown). The posterior communicating arteries (*open arrows*) are seen, as well as symmetric filling of the middle cerebral arteries.

loons, presumably reflecting the various oxidative states of hemoglobin within thrombus. Because of the presence of T1 shortening, portions of the thrombus mimicked residual flowing lumen on the MRA (Figs. 4D and 4E). However, by careful comparison of the SE MR and the source MRA data, residual aneurysm lumen could be detected. It was concluded that there was no gross evidence of interval change between the XRA and MR, and a repeat XRA was not performed.

Patient 5

A 68-year-old woman was evaluated 7 days after two balloons were placed within a giant, partially thrombosed, right supraclinoid internal carotid artery aneurysm. The SE MR (Figs. 5A and 5B) demonstrated mixed intensity laminar thrombus and occlusion balloons. MRA (Figs. 5C and 5D) demonstrated equivocal results in a similar fashion to patient 4, such that it was difficult to distinguish between hyperintense thrombus and the possibility of flow-related enhancement due to slow flow within the residual lumen. Because of the equivocal findings, XRA (Fig. 5E) was performed the next day and demonstrated residual lumenal filling that was completely missed on the MRA.

Discussion

Experience in the use of MR angiography as a tool for the detection and evaluation of intracranial aneurysms (6–8) has been limited. Although promising, the role of MRA in screening the intracranial circulation for aneurysms remains to be defined (8). To our knowledge there is no published data on the use of this new modality as a noninvasive method for post-therapeutic assessment. Patients who have undergone balloon occlusion of intracranial aneurysms are ideal candidates for MR/MRA since the therapeutic balloons used are essentially free of metallic artifact that is associated with intracranial aneurysm clips. Preliminary reports using relatively thick slice two-dimensional Fourier transformation gated cine gradient-recalled echo (GRE) imaging demonstrated the potential use of GRE MR in delineating the results of balloon embolization (9). However, the poor resolution of thick-slice two-dimensional Fourier transformation GRE imaging has limited its widespread use. With the adoption of 3DTOF GRE MRA and sub-cubic millimeter voxel imaging, limitations in spatial resolution have been reduced. The purpose of this report is to present our anecdotal experience using 3DTOF MRA to evaluate subjects who have undergone transcatheter embolization. In some cases, the results were quite satisfactory; however, significant artifacts were encountered in other cases

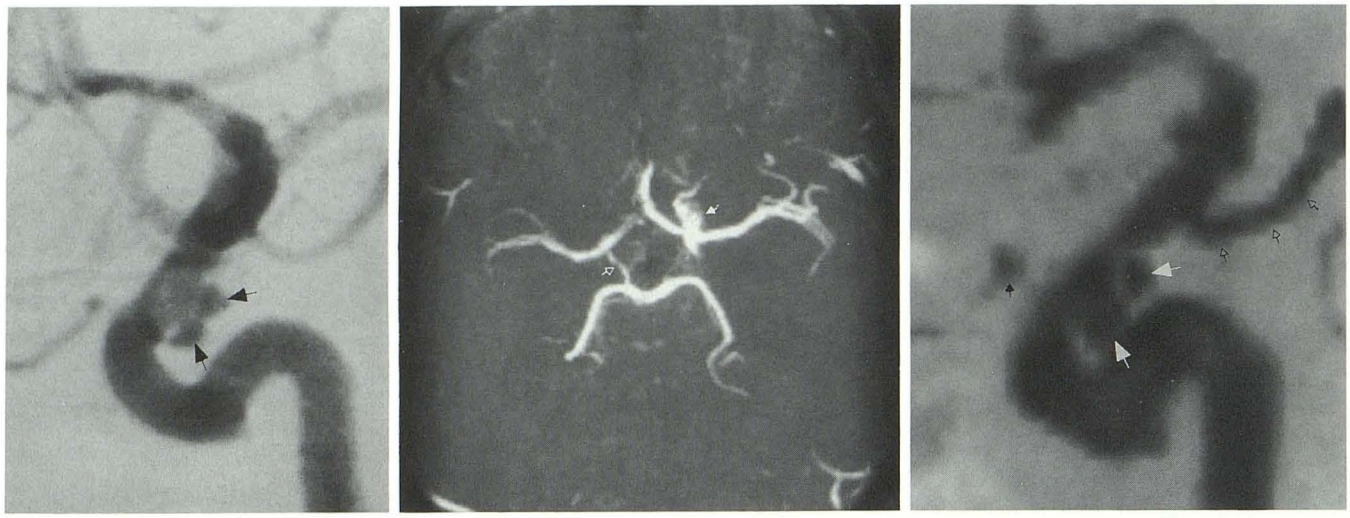

Fig. 3. A 51-year-old woman (patient 3) followed 40 months postocclusion of the right internal carotid artery for a supraclinoid aneurysm. Patient has known untreated aneurysm involving the left carotid-ophthalmic artery. This case demonstrates the utility of MRA in confirming the occlusion of a parent artery and evaluating the circle of Willis, as well as its ability to provide long-term follow-up of a known abnormality.

A, Lateral view, left internal carotid artery XRA depicts a partially thrombosed left posterior carotid-ophthalmic artery aneurysm (*arrows*).

B, Submental vertex MRA collapsed view demonstrates lack of flow-related enhancement in the right internal carotid artery and nonfilling of the treated right internal carotid artery aneurysm. Flow is preserved in the right anterior and middle cerebral arteries. The right posterior communicating artery (*open arrow*) is well visualized. The left internal carotid artery (*solid arrow*) in this projection is within normal limits.

C, Lateral MRA reprojected view of the left internal carotid artery shows the known aneurysm (*large arrows*) in a similar fashion as the XRA. The apparent focal enlargement of the proximal segment of the ophthalmic artery (*small solid arrow*), slightly more prominent on the MRA, is due to slight tortuosity and vessel overlap of the artery in the lateral projection. The posterior communicating artery (*small open arrows*) appears to have increased in size on the postocclusion MRA when compared to the preocclusion XRA (*A*). This finding is presumably due to the recruitment of the left posterior communicating artery as a collateral vessel supplying the contralateral hemisphere.

that can potentially lead to misinterpretation of the results.

Three of the cases (patients 1, 4, and 5) had partially treated aneurysms showing residual flow on XRA. MRA was able to detect this flow in two of these patients with reasonably good correlation. In these two patients with residual flow, no further treatment or repeat XRA was performed. In the third (patient 5), the MRA failed to detect aneurysm flow. The reasons for failure will be discussed below. In the two cases (patients 2 and 3) who had occlusion of the parent internal carotid artery, lack of flow in the parent vessel was confirmed on MRA.

Although the reprojected maximum intensity projection views (Figs. 1E, 3C, and 4E) were used to compare with the XRA, we routinely examined the collapsed maximum intensity projection images (equivalent to the submental vertex view obtained with XRA), as well as all the individual source images from the 3DTOF MRA data sets. The collapsed views (Figs. 2C and 3B) were particularly helpful in providing a unique projection of the circle of Willis, including information on the size and filling of collateral vessels, such as the posterior and anterior communicating arteries, and filling of the proximal anterior and middle cerebral artery branches ipsilateral to the side of carotid occlusion. The individual submillimeter thick source images (Figs. 1D, 4B, and 5C) were useful in providing cross-sectional images that assisted in the localization of the intraaneurysmal balloons with respect to the parent artery and surrounding thrombus and provided detailed information on the adjacent brain parenchyma. Examination of the individual source images also helps evaluate artifacts inherent with maximum intensity projection reconstructions such as overestimation of stenosis and underestimation of vessel diameter (10).

Despite sub-cubic millimeter voxel imaging, limited resolution continues to be a problem. For example, in our experience, we have had variable success with this technique in the visualization of

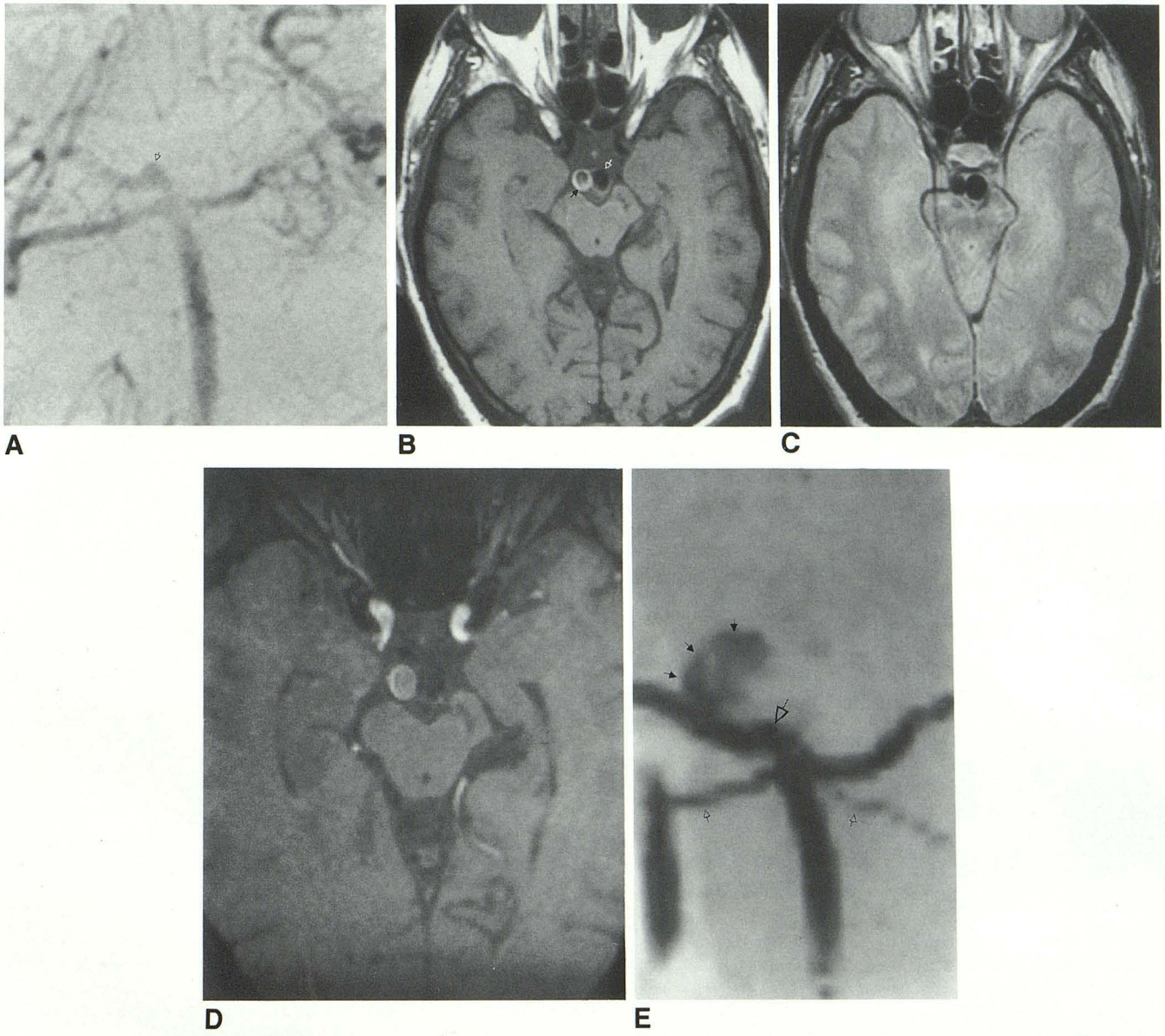

Fig. 4. A 60-year-old man (patient 4) 31 months after intraaneurysmal balloon occlusion of a basilar tip aneurysm using three balloons. This case illustrates the difficulty in determining the patency of a residual aneurysm lumen in the presence of thrombus.

A, Anterior-posterior XRA of the basilar tip depicts a small aneurysm remnant (*open arrow*).

B, Axial T1-weighted (600/20) spin-echo image shows two of the occluding balloons. The one on the left is hypointense (*white open arrow*) while the right balloon (*black solid arrow*) is isointense, with a rind of hyperintensity that was thought to represent subacute thrombus.

C, The first echo (2800/30) of a T2-weighted spin-echo study, at a slightly different level compared to *B*, shows both balloons as areas of hypointensity, simulating flow-related signal void. The rind of hyperintensity is no longer identified and is either hypo- or isointense with the surrounding cerebrospinal fluid. Similar findings were noted on the second echo (2800/80) image (data not shown).

D, Axial partition from MRA shows the right balloon and surrounding thrombus to have similar signal intensity as on the T1-weighted spin-echo image. Due to its increased signal intensity, it was not possible to completely exclude slowly flowing blood in this region based on the MRA study alone.

E, Anterior-posterior MRA reprojected view shows subacute thrombus and hyperintense occluding balloon complex (*small solid arrows*) simulating flow in the right lateral aspect of the aneurysm. The *large open arrow* depicts residual aneurysmal lumen filling from the proximal right posterior cerebral artery in a similar fashion as in *A*. The superior cerebellar arteries (*small open arrows*) are also depicted.

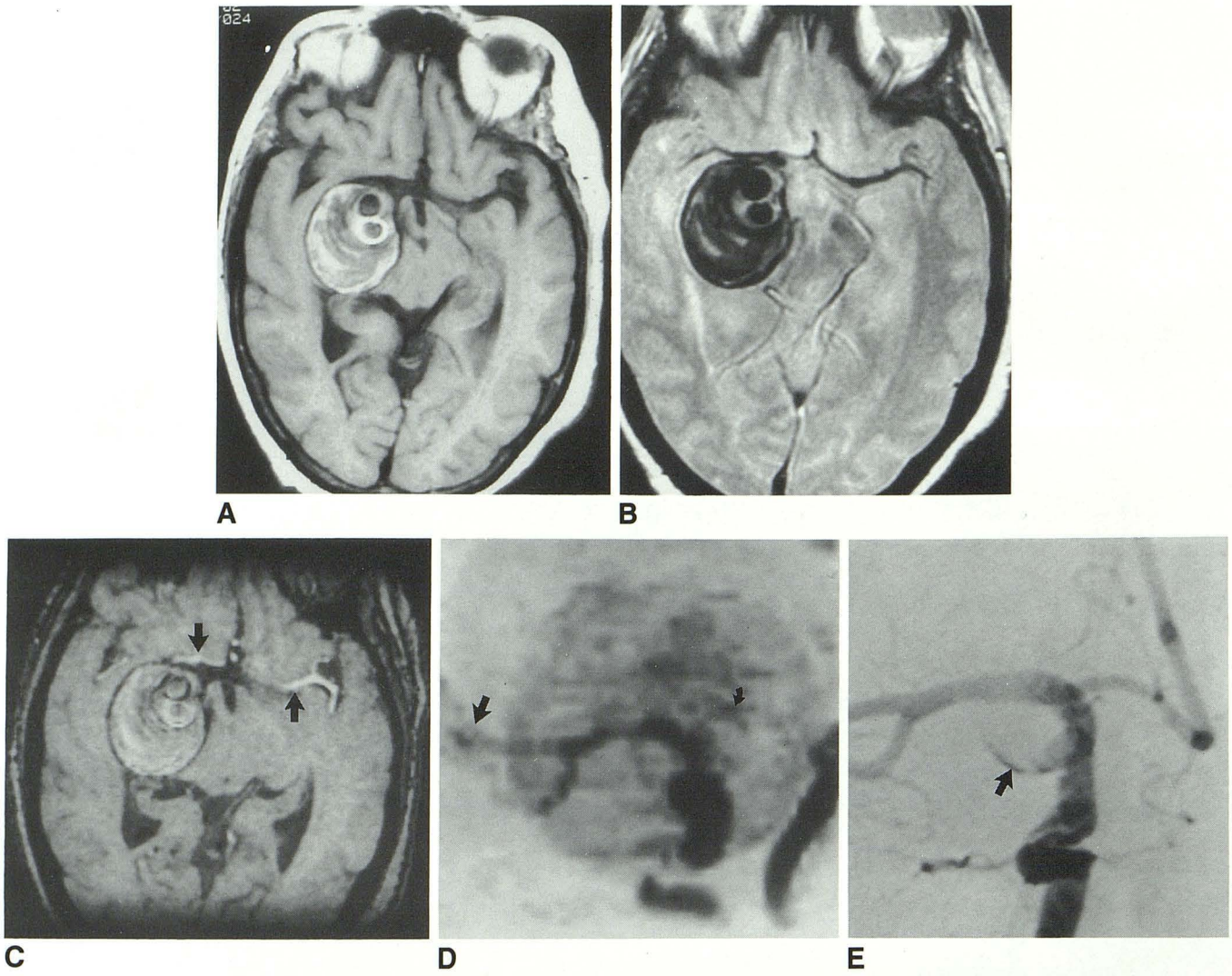

Fig. 5. A 68-year-old woman (patient 5) with giant, largely thrombosed, right supraclinoid internal carotid artery aneurysm, 7 days post-intraaneurysmal occlusion with two detachable balloons. This case depicts the difficulty in distinguishing between complete occlusion from slow flow and hyperintense thrombus.

A, Axial T1-weighted (600/20) spin-echo image shows a giant aneurysm with abundant iso- to hyperintense laminar thrombus surrounding two occlusion balloons, one isointense and one hypointense compared to normal brain parenchyma.

B, Axial T2-weighted (2800/80) spin-echo image shows both balloons to be hypointense and surrounded by iso- to hypointense thrombus.

C, Axial partition from MRA is very similar in appearance to *A*. It is difficult to distinguish between hyperintense thrombus and flow-related enhancement as depicted in the middle cerebral arteries (*arrows*).

D, Anterior-posterior MRA reprojected view depicts the thrombus as a large spherical region of altered intensity. Aneurysm neck and residual lumenal flow could not be defined. Note the signal loss due to saturation effects in the distal middle cerebral artery branches (*straight arrow*) and anterior cerebral artery (*curved arrow*).

E, Anterior-posterior XRA of the right internal carotid artery shows residual lumenal flow inferiorly (*arrow*).

the ophthalmic artery, which is clearly detected in only half of our patients. An example of what is commonly seen with normal ophthalmic arteries using our current technique is shown on Figure 1E. This problem is presumably due to limitations in both spatial and contrast resolution, due to the small size of the vessel, as well as artifactual signal loss due to the dephasing effects from fast or nonconstant blood flow and/or field inhomogeneities. This type of signal loss within a vessel can mimic true stenosis and can be problematic in evaluating collateral blood flow or assessing narrowing of a small branch vessel adjacent to an aneurysm. These inherent problems are of great concern to us when trying to interpret MRA of the circle of Willis. Higher resolution MRA sequences less sensitive to complex flow artifact (4) and improvements in contrast to noise (by

reducing saturation effects) will be required. Recent results using an optimized time-of-flight technique have shown very good correlation with XRA in the visualization of vessels greater than 0.9 mm (11).

The failed study (patient 5) that was encountered points out the two most important limitations of time-of-flight MRA: high-intensity subacute thrombus and slow flow leading to saturation and reduced signal. First, in the presence of the T1-shortening effect due to methemoglobin, subacute thrombus within the aneurysm lumen makes the detection of any adjacent flow-related enhancement difficult since both appear hyperintense on MRA. This hyperintensity is due to the use of relatively T1-weighted GRE sequences that incorporate spoiling gradients for the flow-sensitive acquisition (4). This artifact has been encountered previously in large and giant aneurysms with an abundant amount of thrombus (9). The reprojected images will also show similar artifacts since the maximum intensity projection algorithm (5) cannot discriminate between flow-related enhancement and subacute thrombus. As a result, both entities are simultaneously projected as hyperintensity (Fig. 5D).

Second, the identification of slowly flowing blood may be difficult with time-of-flight MRA. This problem can be understood if one realizes that image contrast on MRA is proportional to velocity (if flow separation and/or turbulence is not present). In the case of slow velocities and/or dilated vascular structures, a prolonged transit time of moving spins through the 3-D volume occurs. Due to this long dwell time, the slowly moving protons receive multiple radio frequency excitations leading to progressive saturation, similar to the stationary protons. Clinically, this problem may occur in patients with reduced intracranial arterial velocities, for example, poor cardiac output, or dilated intracranial vascular structures, such as dolichoectasia or large aneurysms (6, 8).

Steps can be taken to overcome some of these limitations of time-of-flight MRA. First, to avoid misinterpreting subacute thrombus as flow-related enhancement, direct comparison of axial partitions from the MRA study with axial T1-weighted spin-echo images should be done. By using this technique, thrombus should have a similar appearance between the two studies, whereas flow-related enhancement on MRA should be replaced by flow void on the spin-echo study. Care must be taken to avoid any flow-related enhancement artifact on the spin-echo study by using inferior saturation and by placing the region of interest within the center of the imaging volume. An example of using this type of comparison is depicted on Figures 4B and 4D. Despite these precautions, it may not be possible to distinguish between these two phenomena if there is partial volume artifact or in the presence of very slow flow states with reduced flow voids.

While GRE versus T1-weighted spin-echo comparison is the simplest solution to this problem, one could speculate that improved distinction between thrombus and flow may be obtained by using either a rephase/dephase subtraction sequence (12) or phase sensitive imaging in which signal is recovered from moving spins only (13). With these alternative techniques, subacute thrombus should yield no signal; thus, any signal within the aneurysm will represent residual blood flow.

Despite our understanding of the major problems and workable solutions, unambiguous interpretation of time-of-flight MRA in any given patient following EBO therapy may not be possible. This is because our quantitative understanding of the limitations of 3DTOF MRA is incomplete. In instances where it is absolutely critical to distinguish between slow flow and either thrombus or complete occlusion, time-of-flight MRA may not give all the answers. In our practice, the MRA results are always interpreted in conjunction with the patient's history. If the interval history shows clear cut progression of symptoms despite a negative or unchanged MRA, the patient will likely undergo repeat XRA.

In summary, our anecdotal experience with 3DTOF MRA in this patient population has pointed out the deficiencies, as well as potential applications, of this new technique. These initial results indicate that some of these limitations, such as spatial resolution, insensitivity to slow-flow states, and subacute thrombus artifacts, need to be addressed before there is widespread adoption of this technique. From this initial learning experience, we have revised our MRA protocols to address some of these limitations including high resolution (512^2) 3DTOF and 3-D phase contrast acquisitions. A more detailed prospective evaluation of these newer techniques compared with XRA is in progress at our institution.

References

1. Serbinenko FA. Balloon catheterization and occlusion of major cerebral vessels. *J Neurosurg* 1974:41:125–145

2. Fox AJ, Vinuela F, Pelz DM, et al. Use of detachable balloons for proximal artery occlusion in the treatment of unclippable cerebral aneurysms. *J Neurosurg* 1987;66:40–46
3. Higashida RT, Halbach VV, Barnwell SL, et al. Treatment of intracranial aneurysms with preservation of the parent vessel: results of percutaneous balloon embolization in 84 patients. *AJNR* 1990;11: 633–640
4. Schmalbrock P, Yuan C, Chakeres DW, Kohli J, Pelc NJ. Volume MR angiography: methods to achieve very short echo times. *Radiology* 1990;175:861–865
5. Laub G. Displays for MR angiography. *Magn Reson Med* 1990;14: 222–229
6. Masaryk T, Modic M, Ross J, et al. Intracranial circulation: preliminary clinical results with three-dimensional (volume) MR angiography. *Radiology* 1989;171:793–799
7. Sevick RJ, Tsuruda JS, Schmalbrock P. Three-dimensional time-of-flight MR angiography in the evaluation of cerebral aneurysms. *J Comput Assist Tomogr* 1990;14:874–881
8. Ross J, Masaryk T, Modic M, Ruggieri P, Haacke E, Selman W. Intracranial aneurysms: evaluation by MR angiography. *AJNR* 1990; 11:449–456
9. Tsuruda JS, Halbach VV, Higashida RT, Mark AS, Hieshima GB, Norman D. MR evaluation of large intracranial aneurysms using cine low flip angle gradient-refocused imaging. *AJNR* 1988;9:415–424
10. Anderson C, Saloner D, Tsuruda J, Shapeero L, Lee R. Artifacts in maximum-intensity-projection display of MR angiograms. *AJR* 1990; 154:623–629
11. Blatter D, Parker D, Robison R. Cerebral MR angiography with multiple overlapping thin slab acquisition. I. Quantitative analysis in vessel visibility. *Radiology* 1991;179:805–811
12. Alfidi RJ, Masaryk TJ, Haacke EM, et al. MR angiography of peripheral, carotid, and coronary arteries. *AJR* 1987;149:1097–1109
13. Spritzer CE, Pelc NJ, Lee JN, Evans AJ, Sostman HD, Riederer SJ. Rapid MR imaging of blood flow with a phase-sensitive, limited-flip-angle, gradient recalled pulse sequence: preliminary experience. *Radiology* 1990;176:255–262